Revisiting Factorizing Aggregated Posterior in Learning Disentangled Representations

Ze Cheng 12 Juncheng Li 23 Chenxu Wang 1 Jixuan Gu 45 Hao Xu 46 Xinjian Li 3 Florian Metze 3

Abstract

In the problem of learning disentangled representations, one of the promising methods is to factorize aggregated posterior by penalizing the total correlation of sampled latent variables. However, this well-motivated strategy has a blind spot: there is a disparity between the *sampled* latent representation and its corresponding *mean* representation. In this paper, we provide a theoretical explanation that low total correlation of sampled representation cannot guarantee low total correlation of the mean representation. Indeed, we prove that for the multivariate normal distributions, the mean representation with arbitrarily high total correlation can have a corresponding sampled representation with bounded total correlation. We also propose a method to eliminate the above-mentioned disparity. Experiments show that our model can learn a mean representation with much lower total correlation, hence a factorized mean representation. Moreover, we offer a detailed explanation of the limitations of factorizing aggregated posterior: factor disintegration. Our work indicates a potential direction for future research of disentangled learning.

Disentangled representation is believed to be the key to learn a better representation (Bengio et al., 2013; LeCun et al., 2015; Peters et al., 2017). There are 2 major ingredients of disentanglement: 1. Models should learn separate factors of variations (Bengio et al., 2013); 2. Factors should be compact (Bengio et al., 2013), informative and independent from task at hand (Goodfellow et al., 2009). The motivation of disentanglement includes usefulness for downstream tasks (Bengio et al., 2013), being invariant to nuisance factors

(Kumar et al., 2017), improving robustness to adversarial attack (Alemi et al., 2016), etc. (See also the introduction of disentangled representation in Locatello et al. (2018); Chen et al. (2018); Kim and Mnih (2018) and reference therein.)

Recent works (Higgins et al., 2017; Kim and Mnih, 2018; Chen et al., 2018; Kumar et al., 2017; Ridgeway and Mozer, 2018) have introduced various regularizers to the objective function of the Variational Autoencoder (VAE) (Kingma and Welling, 2013; Bengio et al., 2007), Evidence Lower Bound (ELBO). They aim at factorizing aggregated posterior, $q(z) = \int q(z|x)p(x)dx$, which hopefully can encourage disentanglement. Among these works, Kim and Mnih (2018); Chen et al. (2018) independently proposed a promising regularizer, the total correlation (TC) of sampled representation. TC is defined to be the KL-divergence between the joint distribution $\mathbf{z} \sim q(z)$ and the product of marginal distributions $\prod_i q(z_i)$. The TC of a sampled representation, TC_{sample} , should describe its level of independence. In this case, a low value suggests a more factorized joint distribution.

However, Locatello et al. (2018) point out, though these works seem to be effective at factorizing aggregated posterior, there exists a blind spot: a disparity between TC_{sample} and the TC of the corresponding mean representation, TC_{mean} . Specifically, A low TC_{sample} does not necessarily give rise to a low TC_{mean} . Conventionally, the mean representation is used as the encoded latent variables, an unnoticed high TC_{mean} is usually the culprit behind the undesirable entanglement. They found that as the strength of regularization on TC_{sample} increases, TC_{sample} decreases as expected, but TC_{mean} increases. Moreover, the scores under disentanglement metrics are uncorrelated to the regularization strength. Their finding has 2 implications:

- 1. Low TC_{sample} does not imply low TC_{mean} , which is yet not understood;
- 2. Either low TC_{sample} or low TC_{mean} does not guarantee disentanglement. Disentanglement does not seem to correlate with TC_{sample} or TC_{mean} no matter how much these 2 quantities change.

This created several important yet not answered questions:

¹Bosch China Investment Ltd ²Bosch Center for AI ³School of Computer Science, Carnegie Mellon University ⁴Work as intern in Bosch China ⁵School of Mathematical Sciences, Shanghai Jiaotong University ⁶Department of Applied Mathematics, University of Colorado at Boulder. Correspondence to: Ze Cheng <ze.cheng@cn.bosch.com>.

Why does TC_{sample} have no control over TC_{mean} ? Is the strategy of regularizing TC unhelpful to disentanglement? In this paper, we answer the first question completely by theoretically analyzing the relation between TC_{sample} and TC_{mean} . Then after investigating factorized representations, we believe that regularizing TC still might be a key to learning disentangled representation and hopefully our study can shed some light into this problem.

Our main contributions are listed as the followings:

- We prove that for all mean representations in multivariate normal distribution, there exists a large class of sample distributions with bounded TC (See Theorem 1). This implies that a low TC of sample distribution cannot guarantee a low TC of mean representation. (Section. 2)
- We show how to control both TC_{sample} and TC_{mean} and obtain factorized mean representation. Our method is to introduce a simple yet effective regularizer, a penalty term on the *variance* of each latent variable, which forces a sampled representation to behave similarly to the corresponding mean representation. (Section. 3)
- We compare different methods of TC estimation and point out that the method of minibatch estimators (MSS/MWS) suffers from the curse of dimensionality, i.e., the estimation accuracy decays significantly with the increase of the dimension of the latent space. In addition, they may cause unintended shutdown of latent dimensions. (Section. 4)
- We investigate the limitation of factorized mean representation and suggest a tradeoff be considered for the future work of learning disentangled representation. (Section. 5)

1. Related Works

VAE (Kingma and Welling, 2013; Bengio et al., 2007) takes the variational approach to approximate the posterior p(z|x) with q(z|x) by minimizing their KL-divergence, $\mathrm{KL}(q(z|x)||p(z|x))$, which is equivalent to maximizing ELBO. As a result, the high-dimensional real world observations $\mathbf x$ is encoded into lower-dimension latent variable $\mathbf z$ that is expected to be semantically meaningful.

In order to learn disentangled representation, Higgins et al. (2017) proposed a modification of the VAE framework and introduced an adjustable hyperparameter β that balances latent channel capacity and independence constraints with reconstruction accuracy.

Chen et al. (2018) proposed β -TCVAE which adopts the idea of decomposing the average ELBO (Hoffman and John-

son, 2016) and penalizes the TC of latent variables aiming on regularizing a more precise source of disentanglemnet. Around the same time, Kim and Mnih (2018) proposed a similar regularizer penalizing TC_{sample} called FactorVAE. The major difference between FactorVAE and β -TCVAE lies in their different strategies of estimating TC_{sample} . Chen et al. (2018) used formulated estimators while Kim and Mnih (2018) utilized the density-ratio trick which requires an auxiliary discriminator network. We will discuss these two strategies more in details in Section. 4. Kumar et al. (2017) introduced DIP-VAE-I&II, which penalize on the covariance matrix of mean and sampled latent variables respectively in order to encourage disentanglement. This strategy could learn an uncorrelated but not independent distribution.

Locatello et al. (2018) challenged most recent work on disentanglement and argued that unsupervised learning of disentangled representations without inductive biases is basically impossible. This makes strong suggestion that researchers should pay attention to representative learning with inductive biases on both learning approaches and data sets. We refer readers to works in this direction, e.g. Thomas et al. (2018); Bouchacourt et al. (2018); Rolinek et al. (2019) and works referred therein. However, Locatello et al. (2018) does not provide an explanation to one of the observations they made, i.e., why most regularizers are effective at factorizing aggregated posterior but the corresponding mean representations may be entangled? We answer this question in the next section.

2. The Disparity between Total Correlation of Mean and Sampled Distribution

In information theory, total correlation (TC) is one of the generalizations of mutual information (see definition 1), which measures the difference between the joint distribution of multiple random variables and the product of their marginal distributions. A high value of TC indicates the joint distribution is far from an independent distribution, and hence it suggests high entanglement among these random variables.

Definition 1. The total correlation of random variable \mathbf{x} is defined as

$$TC(\mathbf{x}) := KL\left(p(x)||\prod_{j} p(x_{j})\right) = \mathbb{E}_{p(x)}\left[\log \frac{p(x)}{\prod_{j} p(x_{j})}\right].$$

Motivated by this concept, people seek the solution of disentanglement in the form of low TC of the latent variables (Kim and Mnih, 2018; Chen et al., 2018). However, Locatello et al. (2018) pointed out that even though TC_{sample} is low, TC_{mean} can be high. This is problematic because

the mean representation is usually taken as the representation of input and such representation is entangled.

Hence, a clear understanding of the relation between TC_{sample} and TC_{mean} is needed. To this end, we present a theorem that provides an explicit bound for TC_{sample} under some mild assumptions. This bound does not rely on the distribution of mean representation, which turns out to be the root of the disparity between the two TCs. One of the assumptions we made is that the distribution of mean representation is multivariate normal (MVN), but actually the theorem can be easily generalized to distributions with compact support or fast decay. This makes the theorem relatively general and effective for many practical cases.

Here are some notations: μ and z are random variables, and μ and z are corresponding samples (fixed values); Σ and Σ' are matrices; C stands for some constant.

Theorem 1. Let $\mu \sim \mathcal{N}(0, \Sigma)$. For a fixed μ , let $\mathbf{z}|\mu \sim \mathcal{N}(\mu, \Sigma'(\mu))$, where $\Sigma'(\mu)$ is diagonal and satisfies that,

$$c_1 \le \sigma_i'(\mu) \le c_2,\tag{1}$$

where $c_1, c_2 > 0$ and $\sigma'_j(\mu)$ is the diagonal element of $\Sigma'(\mu)$. Then $TC(\mathbf{z})$ is independent of $TC(\mu)$ and

$$TC(\mathbf{z}) \le C \frac{c_3^D}{c_1^D} \log\left(\frac{c_2}{c_1}\right) + C \frac{c_3^{D+2}}{c_1^{D+2}},$$
 (2)

where $c_3 = \max(c_2, \sqrt{D})$ and C is some constant that replies only on dimension D.

The details of the proof are presented in Appendix 2. Intuitively, in the case of multivariate normal distribution, if there exist two dimensions of μ with high correlation, then the TC of this distribution is high (less independent). And the probability density is narrowly distributed in the subspace of these two dimensions. Now, if the standard deviations of $\mathbf{z}|\mu$ corresponding to these two dimensions are suitably large (bounded away from zero), then the distribution of \mathbf{z} will spread wider in the subspace which is closer to a distribution with low TC (more independent). Figure 1 gives an example, for a distribution of μ with high TC, how to construct distribution of \mathbf{z} with low TC.

One fact can be deduced from Theorem 1 is: with a fixed upperbound of $TC_{sample} = TC(\mathbf{z})$ (by fixing parameters c_1, c_2), one can make $TC_{mean} = TC(\boldsymbol{\mu})$ arbitrarily large. To see this, we use Proposition 1 in Section. 4, which states $TC(\boldsymbol{\mu})$ depends only on the determinant of the correlation matrix of $\boldsymbol{\mu}$, i.e., $|\boldsymbol{\Sigma}|$, so we only need to tune the off-diagonal elements of $\boldsymbol{\Sigma}$ (while keeping c_1, c_2 unchanged) to make $|\boldsymbol{\Sigma}|$ go to zero and hence $TC(\boldsymbol{\mu})$ go to infinity.

Interestingly, we note that in Theorem 1 when $c_1 = c_2$ approaches zero, the upperbound of $TC(\mathbf{z})$ goes to infinity. It reflects the following fact: when the distribution of \mathbf{z} is

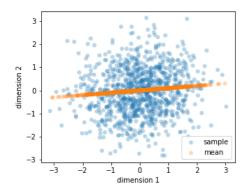


Figure 1. As an example of disparity between mean and sampled representation, consider the following $\boldsymbol{\mu}$ and \mathbf{z} . Let $(\boldsymbol{\mu}_1,\boldsymbol{\mu}_2) \sim \mathcal{N}(0,\boldsymbol{\Sigma})$, where $\boldsymbol{\Sigma} = \begin{pmatrix} 1 & 0.1 \\ 0.1 & 0.01 \end{pmatrix}$, then $TC_{mean} = TC(\boldsymbol{\mu}_1,\boldsymbol{\mu}_2) = \infty$. Note that $\boldsymbol{\mu}_1$ has almost shut down. Also, let $\mathbf{z}_1|\boldsymbol{\mu}_1 \sim \mathcal{N}(\boldsymbol{\mu}_1,0.01)$ and $\mathbf{z}_2|\boldsymbol{\mu}_2 \sim \mathcal{N}(\boldsymbol{\mu}_2,1)$, then $TC_{sample} = TC(\mathbf{z}_1,\mathbf{z}_2)$ is very low. Such problem (high TC_{mean} and low TC_{sample}) exists in β -TCVAE and FactorVAE.

closed to the distribution of μ , $TC(\mathbf{z})$ is close to $TC(\mu)$, which can be large.

Thus, Theorem 1 provides an explanation to the disparity observed by Locatello et al. (2018) that $TC(\mathbf{z})$ is low but $TC(\boldsymbol{\mu})$ is high. Indeed, for every distribution of $\boldsymbol{\mu}$ with large $TC(\boldsymbol{\mu})$ there exist a family of distributions of $\mathbf{z}|\boldsymbol{\mu}$ with bounded $TC(\mathbf{z})$. If the objective function only penalizes $TC(\mathbf{z})$, the optimization process could easily find a distribution of $(\boldsymbol{\mu}, \mathbf{z})$ with low $TC(\mathbf{z})$ but high $TC(\boldsymbol{\mu})$. However, this disparity can be eliminated. In Section. 3, we propose a simple regularizer to serve this goal.

3. An Additional Regularizer

To simplify notation, let $p(n) = p(x_n)$, $q(z|n) = q(z|x_n)$ and $p(n|z) = p(x_n|z)$. Recall the average *evidence lower bound* (ELBO):

ELBO :=
$$\mathbb{E}_{p(n)} \left[\mathbb{E}_{q(z|n)} [\log p(n|z)] - \text{KL}(q(z|n) || p(z)) \right],$$
(3)

where the first term can be interpreted as *reconstruction error*. Inspired by ELBO decomposition (Hoffman and Johnson, 2016), Chen et al. (2018) refined the decomposition and separated TC of z from other terms. Since the independence of latent variables can be one of the sources of disentanglement, they introduced β -TCVAE with a new objective function that penalizes TC in order to learn factorized representation. At the same time, also recognizing the importance of TC in factorizing aggregated posterior, Kim and Mnih (2018) independently introduced FactorVAE that penalizes TC(z) with a different implementation. Such

strategy of penalizing $TC(\mathbf{z})$ can be formulated as

$$\mathcal{L}_{\beta-\mathrm{TC}} := \mathrm{ELBO} - \beta \mathrm{TC}(z).$$
 (4)

Though this strategy are effective at factorizing aggregated posterior (Locatello et al., 2018), according to Theorem 1 the mean representations can still be entangled. To resolve this, we propose a regularized TC-VAE (RTC-VAE),

$$\mathcal{L}_{\text{RTC}} := \mathcal{L}_{\beta-\text{TC}} - \eta \cdot \text{tr}(\mathbb{E}_{p(n)}Cov_{q(z|n)}[z]), \quad (5)$$

where $\operatorname{tr}(\mathbb{E}_{p(n)}Cov_{q(z|n)}[z]) = \sum_{k}^{D} \mathbb{E}_{p(n)}[\sigma_{k}^{2}(n)]$. Our penalty originates from the first term of the law of total covariance:

$$Cov_{q(z)}[z] = \mathbb{E}_{p(n)}Cov_{q(z|n)}[z] + Cov_{p(n)}(\mathbb{E}_{q(z|n)}[z]).$$

Note that a factorized distribution q(z) must have a diagonal covariance matrix $Cov_{q(z)}[z]$. For VAEs, it is conventional to set q(z|n) as a factorized distribution, e.g. $\mathcal{N}(\mu(n), \operatorname{diag}\sigma^2(n))$, which forces VAEs to behave similar to PCA (Rolinek et al. (2019)). As a result, the first term $\mathbb{E}_{p(n)}Cov_{q(z|n)}[z]$ is forced to be diagonal.

Motivated by this, Kumar et al. (2017) proposed DIP-VAEs which penalizes the off-diagonal terms in the second term in the law of total correlation and ignores the first term in order to get a diagonal covariance matrix $Cov_{q(z)}[z]$. Locatello et al. (2018) recognized DIP-VAEs being effective on factorizing aggregated posterior, but we point out that this is actually mistaken. The reason is simply because zero correlation does not necessarily imply independence (see details in Section 5).

Our approach, on the other hand, does not penalize directly on μ . Instead, we penalize on σ , the standard deviation of the distribution q(z|n), which is the first term in the law of total covariance. This may seem little counter-intuitive at first sight, since penalizing a diagonal component of covariance $Cov[\mathbf{z}] = Cov_{q(z)}[z]$ seems not helpful to factorising. However, in the view of Theorem 1, the additional regularizer in equation 5 will force the distribution of \mathbf{z} to be similar to the distribution of μ . Hence, it pushes us away from the situation of large $TC(\mu)$ and low $TC(\mathbf{z})$. Consequently, by minimizing $TC(\mathbf{z})$ we get low $TC(\mu)$, which leads to factorized mean representations.

In practice, we keep $\operatorname{tr}(\mathbb{E}_{p(n)}Cov_{q(z|n)}[z])$ in a range, e.g., (0.01,0.04), by multiplying the hyperparameter η with 1.2 if this term is greater than 0.04 and set η to zero if the term is smaller than 0.01. If the variance of latent variables vanishes completely, the VAE degenerates to a deterministic autoencoder. Thus, this approach saves the effort of tuning extra hyperparameter and keeps the stochastic nature of VAE.

4. Estimation of Total Correlation

To calculate the objective function equation 5, a key step is to estimate TC. For multivariate normal distribution¹, its ground truth TC can be explicitly calculated thanks to the following proposition,

Proposition 1. Let $\mathbf{x} \sim \mathcal{N}(0, \mathbf{\Sigma})$, then

$$TC(\mathbf{x}) = \frac{1}{2} (\log|\mathrm{diag}(\mathbf{\Sigma})| - \log|\mathbf{\Sigma}|).$$
 (6)

Proposition 1 is a simple result, which is why its exact originality is difficult to track, but it is quite handy in our analysis. In Appendix 3, we provide a simple proof for the convenience of readers. Locatello et al. (2018) even used this proposition to approximate the TC of the mean representations in latent space.

To estimate TC, naive Monte Carlo method comes with an intrinsic issue of underestimation. To resolve this, Kim and Mnih (2018) proposed a discriminator network with the help of *density-ratio trick* (see equation (3) and Appendix D. of Kim and Mnih (2018)). In Chen et al. (2018), two kinds of estimator of TC are proposed, Minibatch Weighted Sampling (MWS) and Minibatch Stratified Sampling (MSS) (see definitions in Appendix 1).

In this work, we adopt density-ratio trick as our main method for estimating the total correlation of RTC-VAE. The reason is that we found out there exist some problems of MWS and MSS: the curse of dimensionality and an unintended latent dimension shutdown.

Our anaysis on MWS and MSS consists of both experimental and theoretic analysis. First, we evaluate MWS, MSS_0 and MSS_1 (see definitions in Appendix 1) through the following experiments. Let $\mu \sim \mathcal{N}(0, \Sigma)$ where $\operatorname{diag}\Sigma = \mathbf{I}$, and $\mathbf{z}|\mu \sim \mathcal{N}(\mu, \Sigma')$ where $\Sigma' = \operatorname{diag}(\sigma^2)$ and $\sigma = 0.1$. We set σ small so that the distribution of \mathbf{z} can be approximated by normal distribution, and the ground truth $\mathrm{TC}(\mathbf{z})$ can be calculated by Proposition 1. Then by adjusting $|\Sigma|$, we can control $\mathrm{TC}(\mathbf{z})$. We evaluate different estimators on different TC's, and results are presented in Figure 2.

From the experiments, we summarize some observations: 1. MWS tends to underestimate TC in general; 2. For latent space of dimension < 4, MSS $_0$ and MSS $_1$ are relatively accurate; 3. For latent space of high dimension, both MSS $_0$ and MSS $_1$ tend to overestimate TC when the actual value of TC is small; 4. Overall MSS $_1$ estimates closer to ground truth than MMS $_0$ does.

In Appendix 1, we provides a theoretic analysis of the 3rd

¹One may choose other prior distributions for a VAE model for different reasons. Here, normal distribution helps our analysis and simplifies the scenario. This is the reason why we choose normal distribution as prior.

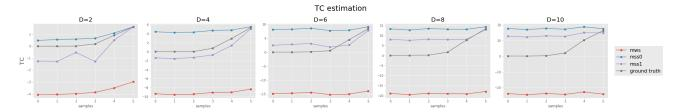


Figure 2. Let $\mu \sim \mathcal{N}(0, \Sigma)$, and $\mathbf{z}|\mu \sim \mathcal{N}(\mu, \Sigma')$ where $\Sigma' = \operatorname{diag}(\sigma^2)$ and $\sigma = 0.1$. The x-axis of each plot shows the determinant of Σ changes from 0 to 1, and y-axis shows $\mathrm{TC}(\mathbf{z})$. Compared with ground truth $\mathrm{TC}(\mathbf{z})$ (calculated by Proposition 1), higher dimension will cause larger error in TC estimation, especially when TC is low.

observation to explain why these estimators deteriorate as dimension increases. In addition, we find that MWS and MSS may lead to an unintended shutdown of latent dimensions. While shutting down dimensions may not necessarily hurt disentanglement (it even can be helpful), the shutdown caused by these estimators is yet less understood for practice. We refer readers to Appendix 1 for detailed analysis.

Density-ratio trick and auxiliary discriminator: The gist of *density-ratio trick* is to estimate the KL-divergence between the distribution of the latent representation q(z) and the distribution of factorized latent representations $\prod_j q(z_j)$, which can be described as following (Nguyen et al., 2010; Sugiyama et al., 2012),

$$TC(\mathbf{z}) \approx \mathbb{E}_{q(z)} \left[\log \frac{D(z)}{1 - D(z)} \right],$$
 (7)

where D is discriminator that classifies \mathbf{z} being sampled from q(z) or $\prod_j q(z_j)$. We implemented our TC estimator according to Section 3 in Kim and Mnih (2018) for training the auxiliary network D.

We do not include a direct numerical comparison between density-ratio trick and MWS/MSS because density-ratio trick would gain unfair advantage due to a potentially overfitting auxiliary discriminator.

5. Experiments

We compare RTC-VAE with three models: FactorVAE and DIP-VAE-I&II. We saved the experiments on β -TCVAE because its problem of disparity is the same as Factor-VAE (Locatello et al., 2018). The datasets we use include dSprites (Matthey et al., 2017), Shapes3D (Burgess and Kim, 2018) and Car3d (Reed et al., 2015). Check Table 2 for the architectures of encoder and decoder and Table 1 for hyper-parameter setting. More details of experiments can be found in Appendix 7. We use the same structure for discriminator as Kim and Mnih (2018) suggested for FactorVAE, which is a 6-layer MLP with 1000 hidden units per layer and leaky ReLU activation.

For RTC-VAE, we set the hyperparameter $\eta = \max(10, \beta)$.

We bound η from below to avoid the situation where the variance term in equation 5 is so small that it will not contribute much compared with the $\mathcal{L}_{\beta-TC}$ term. Especially when β is small, we need η strong enough to regularize TC_{sample} .

We choose batch size 500 for all models on all data sets to balance between performance and training time, whereas Locatello et al. (2018); Kim and Mnih (2018) used 64, Kumar et al. (2017) used 400 and Chen et al. (2018) used 2048 to account for the bias in minibatch estimation. Learning rate is fixed to 1×10^{-3} . We evaluate models on 5000 randomly sampled data on every data set.

We estimate TC_{mean} and TC_{sample} by Proposition 1 as proposed by Locatello et al. (2018). Specifically, we calculate the correlation matrices of the mean and sampled latent vectors, μ 's and z's, encoded from the 5000 samples.

5.1. Eliminating the Disparity between TC_{sample} and TC_{mean}

We first show that RTC-VAE has eliminates the disparity between TC_{sample} and TC_{mean} . Again, since β -TCVAE has the same problem of disparity as FactorVAE, it is sufficient to compare RTC-VAE with FactorVAE. In order to do that, we evaluate TC_{sample} and TC_{mean} of RTC-VAE under different regularization strength and compare them with the corresponding values of FactorVAE.

In Figure 3, we see that: (Left) Under all regularization strength, the disparity exists between TC_{mean} and TC_{sample} for both β -VAE and FactorVAE. (Right) With the regularizer on variance of q(z|n), there is almost no difference between TC_{sample} and TC_{mean} , i.e., the disparity is evidently remedied. In Figure 4, the revised β -VAE and FactorVAE can obtain much lower TC_{mean} and than vanilla ones, meanwhile their TC_{sample} are comparably low.

5.2. Factorizing Aggregated Posterior

Locatello et al. (2018) reported that DIP-VAEs seem to be immune to the disparity between TCs and pointed out it is due to the measurement of TC being Gaussian based.

 $z_0 \& z_9$

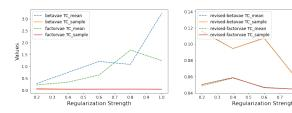


Figure 3. Results on dSprites under all regularization strength: (Left) The disparity exists between dashed lines TC_{mean} and solid lines TC_{sample} for both β -VAE and FactorVAE. (Right) For revised models, the disparity is eliminated.

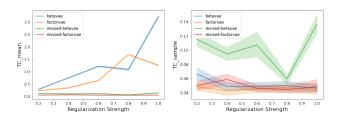


Figure 4. Results on dSprites: (Left) TC_{mean} of revised models are much lower than vanilla models. (Right) TC_{sample} of revised models are comparable to vanilla ones.

Since DIP-VAEs are trained by regularizing the off-diagonal elements of correlation matrix, by Proposition 1 they are guaranteed to have low estimated TCs. Then the question is: Do DIP-VAEs obtain really factorized representation? Our investigation shows that the answer is no.

In Figure 5 (c) and also Figure 6, we see that the learned latent representations of DIP-VAEs are uncorrelated but not factorized. Notice that estimating TC by Proposition 1 is only valid for the multivariate normal distribution. If the presumption is violated, any uncorrelated distribution will have zero TC by such estimation. Since DIP-VAEs penalize directly on the correlation of mean representations, it leads to uncorrelated distributions and low TC estimation. Yet an uncorrelated and non-Gaussian distribution is not necessarily independent or factorized.

On the other hand, RTC-VAE can successfully factorize representations (both sample and mean). Since the mean and sampled representation are very close, we only need to examine one of them. A typical distribution of latent variables learned by RTC-VAE is presented in the pairplot of all latent variables, see Figure 5 (d) and also Figure 15 in Appendix 7. We observe that the distribution present features of discrete independent distributions.

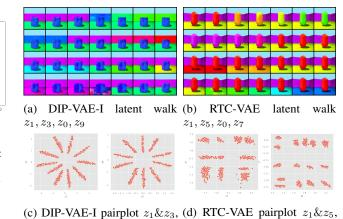


Figure 5. Each row is a latent walk of one dimension of a VAE in (a) and (b). (a) In a DIP-VAE-I model, both $z_1\&z_3$ represent wall hue, and both $z_0\&z_9$ represent floor hue. Notice that each dimension covers different subsets of wall hue or floor hue, even though they are almost uncorrelated (see (c)). (b) In an RTC-VAE model, both $z_1\&z_5$ represent object hue, and both $z_0\&z_7$ represent floor hue, though these dimensions are almost independent (see (d)). (c) Pairplots of $z_1\&z_3$, $z_0\&z_9$ of DIP-VAE show that their correlation is very low (due to its radial symmetry), but they are apparently not independent. (d) The pairplots of $z_1\&z_5$, $z_0\&z_7$ of

RTC-VAE are very close to the behavior of discrete independent

 $z_0 \& z_7$

5.3. Factor Disintegration: Is Factorized Representation Disentangled?

distributions. See full pairplots in Appendix 7.

Now that we can obtain factorized representations, the next question is: is a factorized representation disentangled? Here, we point out *factor disintegration*, indicating multiple *independent* latent variables simultaneously represent one single factor of variation, exists in factorized representation, which maybe an unwanted feature for disentanglement. To this end, future study of disentangled representation should consider this tradeoff between factor disintegration and factorized representations.

First, we will describe what factor disintegration is. For example, in Shape3D, the wall hue is a 1-d factor taking values between 0 and 1. It turns out that a VAE model can cause the 1-d factor to disintegrate into 2 or more latent variables. Then each latent variable controls a subset of wall hue. In this way, even though the VAE can have a highly factorized latent representation, it manages to use multiple dimensions to represent the wall hue instead of one, hence a factor disintegration (see Figure 5 (b) and (d)).

Factor disintegration disobeys the notion of "compactness" introduced by Eastwood and Williams (2018), where compactness indicates each factor associates only one or a few latent variables. So, factor disintegration is a subclass of non-compactness (additionally presuming independence).

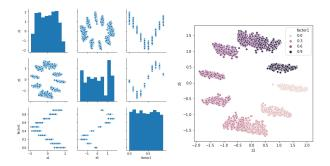


Figure 6. DIP-VAE-I on Shape3D. (Left) Though z_1 is almost uncorrelated to z_5 , they are not independent. Meanwhile, both z_1 and z_5 are clearly linked to factor 1. (Right) A closer look, z_1 and z_5 together represent factor 1, uncorrelated but not independent.

Though there is still disagreement on whether compactness should be a character of disentanglement, e.g., Ridgeway and Mozer (2018), factor disintegration can potentially lead to unnecessarily many latent variables associating to a single factor of variation.

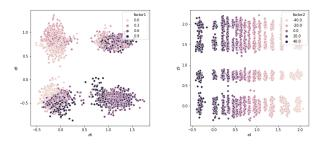


Figure 7. A close look at the factorized latent distribution of RTC-VAE on Shapes3D. Each graph is a distribution of two latent variables, and the color labels how a factor of variation changes. (Left) Affected by factor disintegration, Factor 1 (object hue) has top 2 R^2 scores with latent variables, \mathbf{z}_6 and \mathbf{z}_8 , 0.23 and 0.17 respectively. Meanwhile, \mathbf{z}_6 and \mathbf{z}_8 appear to be independent, and their correlation coefficient $corr(\mathbf{z}_6, \mathbf{z}_8) = 0.017$. (Right) Factor 2 (orientation) is separately represented by \mathbf{z}_4 , and the second top 2 correlated latent variable is \mathbf{z}_9 , and the corresponding R^2 scores are 0.97 and 1×10^{-4} . $corr(\mathbf{z}_4, \mathbf{z}_9) = -0.01$. Then Factor 1 and 2 contribute 0.06 and 0.97 respectively to SAP score.

5.4. The Effect of Factor Disintegration on Disentanglement Metric

To further demonstrate how factor disintegration will affect disentangled learning, we analyze its effect on disentanglement metric.

There are many disentanglement metrics, and most of these metrics share something in common. They look for the link between each factor of variation and each latent variable though the way of measuring the link differs. For exam-

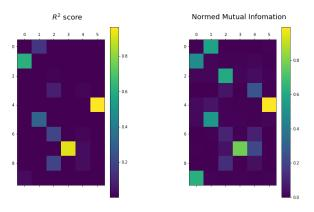


Figure 8. Evaluating an RTC-VAE model with \mathbb{R}^2 scores and normalized mutual information on Shape3D, which are used to calculate SAP and MIG respectively. Columns are factors of variation (ground truth), and rows are latent variables. When the gap between the top 2 scores in a column is small then the metric is suppressed. For example, for factor 1, the highest and second highest scoring variables for both metrics are (z_0, z_5) and the gaps between them are small. (Right) Mutual information discovers more factor disintegration, e.g., factor 0&4 have two high scores and the gaps are small (see Section 5.3). Hence, MIG also gets suppressed (see Section 5.4).

ple, Chen et al. (2018) proposed mutual information gap (MIG), which estimates the mutual information between each latent variable and each ground truth factor and then find the average gap between top 2 scores. DCI (Eastwood and Williams, 2018) computes the uncertainty (entropy) of predicting ground truth factor by latent variables, and then constructs a weighted average as a score. Higgins et al. (2017) proposed BetaVAE, a linear classifier that predicts the index of a fixed factor of variation. Then they use the accuracy of the classifier as a disentanglement metric. Kim and Mnih (2018) improved this method by using majority vote classifier to handle some corner case.

As Locatello et al. (2018) pointed out, most metrics could actually be mildly correlated, and pairs (BetaVAE, Factor-VAE) and (MIG, DCI) are even strongly correlated with each other. It implies that no matter which metric we use, if a model is affected by factor disintegration, it can find multiple latent variables scoring similar values, and hence suppress its final score under such metric.

In the following, we test the argument above with two disentanglement metrics: MIG and Separated Attribute Predictability score (SAP score), proposed by Kumar et al. (2017). Both metrics are classifier-free and essentially independent of the data. The idea behind SAP is similar to MIG but the underline measurement is R^2 score instead of mutual information. Specifically, SAP computes R^2 score between

each latent variable and ground truth factor, and then calculate the difference between top 2 scores for each ground truth factor, and lastly take the average of these differences as a final score. Considering the theoretically optimal case (i.e., every ground truth factor is linearly correlated with exactly one latent variable and uncorrelated with all other variables), SAP score has an optimal value 1 (see evaluation of models with SAP in Appendix 7), whereas MIG is bounded above by the average entropy of each ground truth factor.

In Figure 7 and Figure 8, we see that when factor disintegration happens, the gap between top 2 correlation (with factor) is dramatically suppressed. (see more details in Appendix 7)

6. Conclusion

In this work, we theoretically explain the relation between TC of sampled and mean distribution. We analyze the methods of estimating TC and point out some unnoticed problem. We demonstrate that RTC-VAE can eliminates the disparity between TC of the sampled and mean representations. Also, we compare RTC-VAE with DIP-VAEs and point out that DIP-VAEs can end up with uncorrelated yet dependent latent variables. Last, we find out a tradeoff between factorizing aggregated posterior and factor disintegration underlines disentangling representation.

References

- Alemi, A. A., Fischer, I., Dillon, J. V., and Murphy, K. (2016). Deep variational information bottleneck. *arXiv* preprint arXiv:1612.00410.
- Bengio, Y., Courville, A., and Vincent, P. (2013). Representation learning: A review and new perspectives. *IEEE transactions on pattern analysis and machine intelligence*, 35(8):1798–1828.
- Bengio, Y., LeCun, Y., et al. (2007). Scaling learning algorithms towards ai. *Large-scale kernel machines*, 34(5):1–41.
- Bouchacourt, D., Tomioka, R., and Nowozin, S. (2018). Multi-level variational autoencoder: Learning disentangled representations from grouped observations. In *Thirty-Second AAAI Conference on Artificial Intelligence*.
- Burgess, C. and Kim, H. (2018). 3d shapes dataset. https://github.com/deepmind/3dshapes-dataset/.
- Chen, R. T., Li, X., Grosse, R., and Duvenaud, D. (2018). Isolating sources of disentanglement in vaes. *arXiv* preprint arXiv:1802.04942.
- Eastwood, C. and Williams, C. K. (2018). A framework

- for the quantitative evaluation of disentangled representations.
- Goodfellow, I., Lee, H., Le, Q. V., Saxe, A., and Ng, A. Y. (2009). Measuring invariances in deep networks. In *Advances in neural information processing systems*, pages 646–654.
- Higgins, I., Matthey, L., Pal, A., Burgess, C., Glorot, X., Botvinick, M., Mohamed, S., and Lerchner, A. (2017). beta-vae: Learning basic visual concepts with a constrained variational framework. *ICLR*, 2(5):6.
- Hoffman, M. D. and Johnson, M. J. (2016). Elbo surgery: yet another way to carve up the variational evidence lower bound.
- Kim, H. and Mnih, A. (2018). Disentangling by factorising. *arXiv preprint arXiv:1802.05983*.
- Kingma, D. P. and Welling, M. (2013). Auto-encoding variational bayes. *arXiv preprint arXiv:1312.6114*.
- Kumar, A., Sattigeri, P., and Balakrishnan, A. (2017). Variational inference of disentangled latent concepts from unlabeled observations. *arXiv preprint arXiv:1711.00848*.
- LeCun, Y., Bengio, Y., and Hinton, G. (2015). Deep learning. *nature*, 521(7553):436–444.
- Locatello, F., Bauer, S., Lucic, M., Gelly, S., Schölkopf, B., and Bachem, O. (2018). Challenging common assumptions in the unsupervised learning of disentangled representations. *arXiv preprint arXiv:1811.12359*.
- Matthey, L., Higgins, I., Hassabis, D., and Lerchner, A. (2017). dsprites: Disentanglement testing sprites dataset. https://github.com/deepmind/dsprites-dataset/.
- Nguyen, X., Wainwright, M. J., and Jordan, M. I. (2010). Estimating divergence functionals and the likelihood ratio by convex risk minimization. *IEEE Transactions on Information Theory*, 56(11):5847–5861.
- Peters, J., Janzing, D., and Schölkopf, B. (2017). *Elements of causal inference: foundations and learning algorithms*. MIT press.
- Reed, S. E., Zhang, Y., Zhang, Y., and Lee, H. (2015). Deep visual analogy-making. In *Advances in neural information processing systems*, pages 1252–1260.
- Ridgeway, K. and Mozer, M. C. (2018). Learning deep disentangled embeddings with the f-statistic loss. In *Advances in Neural Information Processing Systems*, pages 185–194.

- Rolinek, M., Zietlow, D., and Martius, G. (2019). Variational autoencoders pursue pca directions (by accident). In *Proceedings of the IEEE Conference on Computer Vision and Pattern Recognition*, pages 12406–12415.
- Sugiyama, M., Suzuki, T., and Kanamori, T. (2012). Density-ratio matching under the bregman divergence: a unified framework of density-ratio estimation. *Annals of the Institute of Statistical Mathematics*, 64(5):1009–1044.
- Thomas, V., Bengio, E., Fedus, W., Pondard, J., Beaudoin, P., Larochelle, H., Pineau, J., Precup, D., and Bengio, Y. (2018). Disentangling the independently controllable factors of variation by interacting with the world. *arXiv* preprint arXiv:1802.09484.

Appendix

1. Problems in Methods of Minibatch Estimators

1.1. Minibatch Weighted Sampling (MWS)

See Chen et al. (2018),

$$\mathbb{E}_{q(z)}[\log q(z)] \approx \frac{1}{M} \sum_{i=1}^{M} \left[\log \sum_{j=1}^{M} q(z(n_i)|n_j) - \log(NM) \right]$$
(8)

1.2. Minibatch Estimators (MSS)

MSS can be described as: For a minibatch of sample, $B_{M+1} = \{n_1, \dots, n_{M+1}\},\$

$$\mathbb{E}_{q(z,n)}[\log q(z)] \approx \frac{1}{M+1} \sum_{i=1}^{M+1} \log f(z_i, n_i, B_{M+1} \setminus \{n_i\}), \tag{9}$$

where

$$f(z, n^*, B_{M+1} \setminus \{n^*\}) = \frac{1}{N} q(z|n^*)$$
(10)

$$+\frac{1}{M}\sum_{m=1}^{M-1}q(z|n_m) + \frac{N-M}{NM}q(z|n_m). \tag{11}$$

 $f(z, n^*, B_{M+1} \setminus \{n^*\})$ is an unbiased estimator of q(z), but it turns out when it is used for estimating TC, it suffers from the curse of dimensions.

 \mathbf{MMS}_0 and \mathbf{MMS}_1 : There is a small part of the implementation of MSS in Chen et al.'s code that is not quite clear to us, specifically, the computation of log importance weight matrix in equation 9. In our experiment, we implement MSS with our understanding and denote it as \mathbf{MSS}_1 , and we denote Chen et al.'s implementation \mathbf{MSS}_0 . The only difference is that we replace this chunk of code (https://github.com/rtqichen/beta-tcvae/blob/master/vae_quant.py#L199-L201) to

```
for i in range(batch_size):
    W[i,i] = 1/N
    W[i,(1+i)%batch_size] = strat_weight
```

1.3. Comparison of the Two Methods

In Section 4 we present our empirical evaluation of MWS, MSS_0 and MSS_1 , and the result is shown in Figure 2. Here, we conduct some theoretical analysis and try to explain some of our observations: For latent space of dimension < 4, MSS_0 and MSS_1 are relatively accurate; for latent space of high dimension, both MSS_0 and MSS_1 tend to overestimate TC when the actual value of TC is small.

Recall the experiment settings: Let $\mu \sim \mathcal{N}(0, \Sigma)$ where $\operatorname{diag}\Sigma = \mathbf{I}$, and $\mathbf{z}|\mu \sim \mathcal{N}(\mu, \Sigma')$ where $\Sigma' = \operatorname{diag}(\sigma^2)$ and $\sigma = 0.1$. We set σ small so that the distribution of \mathbf{z} can be approximated by normal distribution, and the ground truth $\mathrm{TC}(\mathbf{z})$ can be calculated by Proposition 1. Then by adjusting $|\Sigma|$, we can control $\mathrm{TC}(\mathbf{z})$.

1.3.1. THE CURSE OF DIMENSIONALITY

Let M be the batchsize and D be the dimensions of latent space. Notice that $TC(\mu) = 0$ in the above setting and $TC(\mathbf{z})$ is small. Let $TC_{\mathbf{z}}$ be the estimation of $TC(\mathbf{z})$ with minibatch estimator, either equation 9 or equation 8, and we find that for $D \geq 5$ approximately

$$TC_{\mathbf{z}} \approx O((D-1)\log M).$$
 (12)

See details of deduction in Appendix 5. Thus, $TC_{\mathbf{z}}$ seriously overestimates the true $TC(\mathbf{z})$.

1.3.2. Unintended Shutdown of Latent Dimensions

We also find that the estimation of TC by MSS and MWS is lower for distributions with few active latent dimensions (we refer it as dimension "shutdown") than distributions with fully active dimensions. To see why, consider $\mu_0 \sim \mathcal{N}(0, \sigma_0)$, where $\sigma_0 \ll 1$, and $\mu_{0-} \sim \mathcal{N}(0, \mathbf{Id}_{D-1})$ where 0- means all the dimensions except 0, and assume that μ_0 is uncorrelated with the rest, and $\mathbf{z}|\mu \sim \mathcal{N}(0, \mathbf{\Sigma})$, where $\mathbf{\Sigma} = \mathrm{diag}(\sigma^2)$. Again, $TC(\mu) = 0$ and if we choose small σ , $TC(\mathbf{z})$ is small.

Though a similar analysis we find that the estimation of $TC(\mathbf{z})$ is approximately

$$TC_{\mathbf{z}} \approx O((D-2)\log M).$$
 (13)

See a proof in Appendix 6. Compared to equation 12, the distribution with a shutdown dimension has a lower estimation of TC. Hence, by penalizing estimated TC_z a model may converge to distribution with fewer active latent variables.

We note that shutting down latent dimensions may be helpful to learning disentangled representation, e.g., if the number of ground truth dimensions can efficiently represent data, more dimensions may cause entanglement. There are some works studying the phenomenon of dimension shutdown of VAE, and readers may refer to Rolinek et al. (2019) and reference therein. However, in the case of MWS/MSS, the shutdown may be unintended and it is yet unclear exactly how many dimensions get shutdown. In our opinion, in order to precisely induce dimension shutdown, a better solution may be introducing proper bias to models, which also motivates supervised learning to disentangled learning (in addition to regularizing factor disintegration discussed in Section 5.3).

2. Proof of Theorem 1

In the following proof, we follow a convention of mathematical analysis: the meaning of C can change through lines. Specifically, if there are C_1 and C_2 , take $C = \max(C_1, C_2)$. Since we only care about boundedness of some quantity, this notation eliminates some redundant work of tracking. $B_R(c) = \{x \in \mathbb{R}^n : |x - c| < R\}$.

Theorem (Theorem 1 restated). Let $\mu \sim \mathcal{N}(0, \Sigma)$. For a fixed μ , let $\mathbf{z}|\mu \sim \mathcal{N}(\mu, \Sigma'(\mu))$, where $\Sigma'(\mu)$ is diagonal and satisfies that,

$$c_1 \le \sigma_i'(\mu) \le c_2,\tag{14}$$

where $c_1, c_2 > 0$ and $\sigma'_i(\mu)$ is the diagonal element of $\Sigma'(\mu)$. Then $TC(\mathbf{z})$ is independent of $TC(\boldsymbol{\mu})$ and

$$TC(\mathbf{z}) \le C \frac{c_3^D}{c_1^D} \log\left(\frac{c_2}{c_1}\right) + C \frac{c_3^{D+2}}{c_1^{D+2}},$$
 (15)

where $c_3 = \max(c_2, \sqrt{D})$ and C is some constant that replies only on dimension D.

Proof. Let

$$S_{+} = \{ z \in \mathbb{R}^{D} | p(z) \ge \prod_{j} p(z_{j}) \}, \quad S_{-} = \{ z \in \mathbb{R}^{D} | p(z) < \prod_{j} p(z_{j}) \},$$

then

$$\mathrm{TC}(\mathbf{z}) = \int_{S_+} + \int_{S_-} = \mathrm{TC}(\mathbf{z})_+ + \mathrm{TC}(\mathbf{z})_-.$$

Since KL-divergence is non-negative, if $TC(\mathbf{z})_+$ is bounded, then $TC(\mathbf{z})$ must be bounded. In the following, we work on S_+ , i.e., we assume $p(z) \ge \prod_i p(z_i)$.

Note that total correlation is invariant under scaling, i.e., for $\lambda > 0$, $\lambda \mu \sim \mathcal{N}(0, \lambda \Sigma)$, then $TC(\mu) = TC(\lambda \mu)$. In Gaussian case, one can see this by simply applying Proposition 1. Hence, let σ_j be the standard deviation of μ_j , and we can assume $\max_j \sigma_j < 1$. Otherwise we can instead work on $\lambda \mu$ with a sufficient small λ .

Fix some $R \ge 1$, and for |z| < R,

$$\begin{split} p(z) &= \mathbb{E}_{p(\mu)}[p(z|\mu)] = \int_{\mathbb{R}^D} p(\mu) p(z|\mu) d\mu \\ &= \frac{C}{c_1^D} \int_{\mathbb{R}^D} p(\mu) e^{-\frac{1}{2c_2^2}|z-\mu|^2} d\mu \\ &\leq \frac{C}{c_1^D} \int_{\mathbb{R}^D} p(\mu) d\mu \\ &= \frac{C}{c_1^D}, \end{split}$$

And also for |z| < R,

$$\prod_{j} p(z_{j}) \geq \prod_{j} \int_{|\mu_{j}| < R} p(\mu_{j}) \frac{1}{\sqrt{2\pi c_{2}^{2}}} e^{-\frac{(z_{j} - \mu_{j})^{2}}{2c_{1}^{2}}} d\mu_{j}$$

$$\geq \frac{C}{c_{2}^{D}} \int_{|\mu| < R} e^{-\frac{|z - \mu|^{2}}{2c_{1}^{2}}} \prod_{j} p(\mu_{j}) d\mu_{1} \cdots d\mu_{D}$$

$$\geq \frac{C}{c_{2}^{D}} e^{-\frac{2R^{2}}{c_{1}^{2}}} \frac{1}{2^{D}}$$

$$\geq \frac{C}{c_{2}^{D}} e^{-\frac{2R^{2}}{c_{1}^{2}}},$$

where in the second last inequality we use the fact $|z - \mu| < 2R$ and the fact $\max_j \sigma_j < 1$ and $R \ge 1$. Let $\bar{\sigma}$ be the largest singular value of Σ , and for $|z| > R \ge 1$ we have,

$$\begin{split} p(z) &= \int_{B_{\frac{|z|}{2}}(0)} p(\mu) p(z|\mu) d\mu + \int_{B_{\frac{|z|}{2}}(0)} p(\mu) p(z|\mu) d\mu \\ &\leq \int_{B_{\frac{|z|}{2}}(0)} p(\mu) \frac{C}{c_1^D} e^{-\frac{|z-\mu|^2}{2c_2^2}} d\mu + \int_{B_{\frac{|z|}{2}}(0)} p(\mu) \frac{C}{c_1^D} e^{-\frac{|z-\mu|^2}{2c_2^2}} d\mu \\ &\leq \frac{C}{c_1^D} e^{-\frac{||z|-\frac{|z|}{2}|^2}{2c_2^2}} \int_{B_{\frac{|z|}{2}}(0)} p(\mu) d\mu + \frac{C}{c_1^D} \int_{B_{\frac{|z|}{2}}(0)} p(\mu) d\mu \\ &\leq \frac{C}{c_1^D} e^{-\frac{|z|^2}{8c_2^2}} \cdot 1 + \frac{C}{c_1^D} \int_{|\mu| > \frac{|z|}{2}} p(\mu) d\mu \\ &\leq \frac{C}{c_1^D} e^{-\frac{|z|^2}{8c_2^2}} + \frac{C}{c_1^D} \int_{|\tau| > \frac{|z|}{2\bar{\sigma}}} e^{-\frac{|\tau|^2}{2}} d\tau \quad (\text{Let } \tau = T\mu \text{ where } T = (\mathbf{\Sigma}^{-1})^{\frac{1}{2}}) \\ &\leq \frac{C}{c_1^D} e^{-\frac{|z|^2}{8c_2^2}} + \frac{C}{c_1^D} \prod_j \int_{t > \frac{|z|}{2\bar{\sigma}\sqrt{D}}} e^{-\frac{t^2}{2}} dt \\ &\leq \frac{C}{c_1^D} e^{-\frac{|z|^2}{8c_2^2}} + \frac{C}{c_1^D} e^{-\frac{|z|^2}{8D\bar{\sigma}^2}} \left(\frac{|z|}{2\bar{\sigma}\sqrt{D}}\right)^{-D} \\ &\leq \frac{C}{c_1^D} e^{-\frac{|z|^2}{8c_3^2}}, \end{split}$$

where $c_3 = \max(\sigma_2, \sqrt{D}\bar{\sigma})$. The second last inequality is due to the estimation of complementary error function (?). Again, we can scale $\lambda \mu$ such that $\bar{\sigma}$ of $\lambda \Sigma$ is less than 1. Hence, we can set $c_3 = \max(\sigma_2, \sqrt{D})$.

Also for |z| > R,

$$\prod_{j} p(z_{j}) \geq \prod_{j} \left(\int_{|\mu_{j}| < R} p(\mu_{j}) \frac{C}{c_{2}} e^{-\frac{|z_{j} - \mu_{j}|^{2}}{2c_{1}^{2}}} d\mu_{j} \right)
\geq \frac{C}{c_{2}^{D}} \int_{|\mu_{j}| < \sigma_{j}, j = 1...D} e^{-\frac{|z_{j} - \mu_{j}|^{2}}{2c_{1}^{2}}} \prod_{j} p(\mu_{j}) d\mu_{1} \cdots d\mu_{D}
\geq \frac{C}{c_{2}^{D}} e^{-\frac{|z|z|^{2}}{2c_{1}^{2}}} \prod_{j} \left(\frac{1}{2}\right)
\geq \frac{C}{c_{2}^{D}} e^{-\frac{2|z|^{2}}{c_{1}^{2}}}.$$

Thus,

$$\begin{split} &\operatorname{TC}(\mathbf{z}) = \mathbb{E}_{p(z)} \left[\log \frac{p(z)}{\prod_{j} p(z_{j})} \right] \\ &\leq \int_{B_{R}(0)} p(z) \log \frac{p(z)}{\prod_{j} p(z_{j})} dz + \int_{B_{R}^{c}(0)} p(z) \log \frac{p(z)}{\prod_{j} p(z_{j})} dz \\ &\leq \int_{B_{R}(0)} \frac{C}{c_{1}^{D}} \log \left(C \frac{c_{2}^{D}}{c_{1}^{D}} e^{\frac{2R^{2}}{c_{1}^{2}}} \right) dz + \int_{B_{R}^{c}(0)} \frac{C}{c_{1}^{D}} e^{-\frac{|z|^{2}}{8c_{3}^{2}}} \log C \frac{c_{2}^{D}}{c_{1}^{D}} e^{\frac{2|z|^{2}}{8c_{3}^{2}}} \frac{|z|^{2}}{8c_{3}^{2}} dz \\ &\leq \frac{C}{c_{1}^{D}} \log \left(C \frac{c_{2}^{D}}{c_{1}^{D}} e^{\frac{2R^{2}}{c_{1}^{2}}} \right) R^{D} + \int_{B_{R}^{c}(0)} \frac{C}{c_{1}^{D}} e^{-\frac{|z|^{2}}{8c_{3}^{2}}} \left(\log C \frac{c_{2}^{D}}{c_{1}^{D}} + \frac{2|z|^{2}}{c_{1}^{2}} \right) dz \\ &\leq \frac{C}{c_{1}^{D}} \log \left(C \frac{c_{2}^{D}}{c_{1}^{D}} e^{\frac{2R^{2}}{c_{1}^{2}}} \right) R^{D} + \frac{C}{c_{1}^{D}} \log \left(C \frac{c_{2}^{D}}{c_{1}^{D}} \right) \prod_{j} \int_{|z_{j}| > \frac{R}{\sqrt{D}}} e^{-\frac{|z_{j}|^{2}}{8c_{3}^{2}}} dz_{j} + \frac{C}{c_{1}^{D+2}} \int_{|z| > R} e^{-\frac{|z|^{2}}{8c_{3}^{2}}} |z|^{2} dz \\ &\leq \frac{C}{c_{1}^{D}} \log \left(C \frac{c_{2}^{D}}{c_{1}^{D}} e^{\frac{2R^{2}}{c_{1}^{2}}} \right) R^{D} + C \frac{c_{3}^{D}}{c_{1}^{D}} \log \left(C \frac{c_{2}^{D}}{c_{1}^{D}} \right) \frac{e^{-\frac{R^{2}}{8c_{3}^{2}}}}{\left(\frac{R^{2}}{8c_{3}^{2}} \right)^{D}} + \frac{C}{c_{1}^{D+2}} c_{3}^{2} e^{-\frac{R^{2}}{8c_{3}^{2}}} R^{D} \\ &\leq C \frac{c_{3}^{D}}{c_{1}^{D}} \log \left(C \frac{c_{2}^{D}}{c_{1}^{D}} \right) + C \frac{c_{3}^{D+2}}{c_{1}^{D+2}} \quad \text{(Take } R = c_{3} \text{ since it's arbitrary)} \\ &\leq C \frac{c_{3}^{D}}{c_{1}^{D}} \log \left(\frac{c_{2}}{c_{1}^{D}} \right) + C \frac{c_{3}^{D+2}}{c_{1}^{D+2}}. \end{aligned}$$

To estimate the last term in the 4th inequality above, we transform the integral to spherical integral and then repeat integrate-by-part till we can estimate it with complementary error function. \Box

One can directly check that the above argument is valid for $p(\mu)$ with compact support (then c_3 can be taken as c_2) or fast decay (faster than $O(e^{-|\mu|^2})$). Specifically, if $p(\mu)$ has a compact support, the only thing will change is the estimation of p(z) for $|z|>R\geq 1$. Scale μ such that its support is contained in $B_1(0)$. Then the integral on $B_{\frac{|z|}{2}(0)}^c$ is 0 and hence c_3 can take c_2 . If $p(\mu)$ decays faster than $O(e^{-|\mu|^2})$, then the argument is the same.

3. Proof of Proposition 1

Proposition (Proposition 1 restated). Let $\mathbf{x} \sim \mathcal{N}(0, \Sigma)$, then

$$TC(\mathbf{x}) = \frac{1}{2} \left(\log|\operatorname{diag}(\mathbf{\Sigma})| - \log|\mathbf{\Sigma}| \right). \tag{16}$$

Proof. First, recall that the KL-divergence between two distributions \mathbb{P} and \mathbb{Q} is defined as

$$\mathrm{KL}(\mathbb{P}||\mathbb{Q}) = \mathbb{E}_{\mathbb{P}}[\log \frac{\mathbb{P}}{\mathbb{Q}}]$$

Also, the density function for a multivariate Gaussian distribution $\mathcal{N}(\mu, \Sigma)$ is

$$p(x) = \frac{1}{(2\pi)^{n/2} \det(\mathbf{\Sigma})^{1/2}} \exp(-\frac{1}{2}(x-\mu)^T \mathbf{\Sigma}^{-1}(x-\mu)).$$

Now, for two multivariate Gaussian \mathbb{P}_1 and \mathbb{P}_2 , we have

$$\begin{split} \mathrm{KL}(\mathbb{P}_{1}||\mathbb{P}_{2}) &= \mathbb{E}_{\mathbb{P}_{1}}[\log\mathbb{P}_{1} - \log\mathbb{P}_{2}] \\ &= \frac{1}{2}\log\frac{\det\mathbf{\Sigma}_{2}}{\det\mathbf{\Sigma}_{1}} + \frac{1}{2}\mathbb{E}_{p_{1}(x)}[-(x-\mu_{1})^{T}\mathbf{\Sigma}_{1}^{-1}(x-\mu_{1}) + (x-\mu_{2})^{T}\mathbf{\Sigma}_{2}^{-1}(x-\mu_{2})] \\ &= \frac{1}{2}\log\frac{\det\mathbf{\Sigma}_{2}}{\det\mathbf{\Sigma}_{1}} + \frac{1}{2}\mathbb{E}_{p_{1}(x)}[-\mathrm{tr}(\mathbf{\Sigma}_{1}^{-1}(x-\mu_{1})(x-\mu_{1})^{T}) + \mathrm{tr}(\mathbf{\Sigma}_{2}^{-1}(x-\mu_{2})(x-\mu_{2})^{T})] \\ &= \frac{1}{2}\log\frac{\det\mathbf{\Sigma}_{2}}{\det\mathbf{\Sigma}_{1}} - \frac{1}{2}\mathrm{tr}(\mathbf{\Sigma}_{1}^{-1}\mathbf{\Sigma}_{1}) + \frac{1}{2}\mathbb{E}_{p_{1}(x)}[\mathrm{tr}(\mathbf{\Sigma}_{2}^{-1}((xx^{T} - 2x\mu_{2}^{T} + \mu_{2}\mu_{2}^{T}))] \\ &= \frac{1}{2}\log\frac{\det\mathbf{\Sigma}_{2}}{\det\mathbf{\Sigma}_{1}} - \frac{n}{2} + \frac{1}{2}\mathbb{E}_{p_{1}(x)}[\mathrm{tr}(\mathbf{\Sigma}_{2}^{-1}((x-\mu_{1})(x-\mu_{1})^{T} + \underbrace{2(x-\mu_{1})\mu_{1}}_{\mathbb{E}_{p_{1}(x)}(x)=\mu_{1}} + \mu_{1}\mu_{1}^{T} - 2x\mu_{2}^{T} + \mu_{2}\mu_{2}^{T}))] \\ &= \frac{1}{2}\log\frac{\det\mathbf{\Sigma}_{2}}{\det\mathbf{\Sigma}_{1}} - \frac{1}{2}n + \frac{1}{2}\mathrm{tr}(\mathbf{\Sigma}_{2}^{-1}(\mathbf{\Sigma}_{1} + (\mu_{2} - \mu_{1})(\mu_{2} - \mu_{1})^{T})) \\ &= \frac{1}{2}(\log\frac{\det\mathbf{\Sigma}_{2}}{\det\mathbf{\Sigma}_{1}} - n + \mathrm{tr}(\mathbf{\Sigma}_{2}^{-1}\mathbf{\Sigma}_{1}) + (\mu_{2} - \mu_{1})^{T}\mathbf{\Sigma}_{2}^{-1}(\mu_{2} - \mu_{1})) \end{split}$$

Let \mathbb{P} be a multivariate Gaussian $\mathcal{N}(\mu, \Sigma_1)$, and then the product of the marginal distribution $\prod_i p_i(x)$ is also Gaussian $\mathcal{N}(\mu, \Sigma_2)$, where $\Sigma_2 = \operatorname{diag}(\Sigma_1)$. Thus, the total correlation of multivariate Gaussian distribution is

$$TC(\mathbf{x}) = KL(p(x)||\prod_{i} p_{i}(x))$$

$$= \frac{1}{2} (\log \frac{\det \mathbf{\Sigma}_{2}}{\det \mathbf{\Sigma}_{1}} - n + \operatorname{tr}(\mathbf{\Sigma}_{2}^{-1} \mathbf{\Sigma}_{1}) + (\mu - \mu)^{T} \mathbf{\Sigma}_{2}^{-1} (\mu - \mu))$$

$$= \frac{1}{2} (\log \frac{\det \mathbf{\Sigma}_{2}}{\det \mathbf{\Sigma}_{1}} - n + n)$$

$$= \frac{1}{2} (\log |\operatorname{diag}(\mathbf{\Sigma}_{1})| - \log |\mathbf{\Sigma}_{1}|)$$

4. Proof of equation 17

Proof. For t > 0,

$$\begin{split} P(|z^{(i)} - \mu^{(j)}| < t) &= P(|x| < t) \text{ where } x \sim \mathcal{N}(0, 2) \\ &= \int_{-t}^{t} \frac{1}{\sqrt{4\pi}} e^{-\frac{x^2}{4}} dx \\ &= \sqrt{\int_{-t}^{t} \frac{1}{\sqrt{4\pi}} e^{-\frac{x^2}{4}} dx} \int_{-t}^{t} \frac{1}{\sqrt{4\pi}} e^{-\frac{y^2}{4}} dy \\ &= \sqrt{\int_{-t}^{t} \int_{-t}^{t} \frac{1}{4\pi} e^{-\frac{x^2+y^2}{4}} dx dy} \\ &= \sqrt{\int_{0}^{2\pi} \int_{0}^{t} \frac{1}{4\pi} e^{-\frac{r^2}{4}} r dr d\theta} \\ &= \sqrt{1 - e^{-\frac{t^2}{4}}} \\ &= \frac{t}{2} + O(t^2) \end{split}$$

5. Sketched Proof of equation 12

The following argument provides an approximated estimation of related quantities. The goal is not complete rigorousness but rather an intuitive yet quantitative explanation of our observations in Section 4.

Recall that $TC(\boldsymbol{\mu})=0$ and $\sigma=0.1$, and hence $TC(\mathbf{z})$ is small. M is batchsize and D is latent dimension. Now, consider $q(z_k^{(i)}|n^{(j)})$, where (i,j,k) are indices of a box (minibatch, minibatch, dimension) with size $M\times M\times D$ and let $n^{(j)}$ be a sample drawn in a minibatch and $z^{(i)}:=z(n^{(i)})$. We claim: when the ground truth $TC(\mathbf{z})$ is low,considering $q(z_k^{(i)}|n^{(i)})$, only the elements on the diagonal plane of an index-box, namely those probabilities with indices (i,i,k), take some bounded values O(1), and all the other elements are very small.

To rationalize our claim, it is obvious that $q(z_k^{(i)}|n^{(i)})$ is not small, and we only need to show the probability of $q(z_k^{(i)}|n^{(j)})$, $i \neq j$, being large is small enough to ignore for each minibatch. Let us first consider 1-D cases, where $\mu \sim \mathcal{N}(0,1)$, $\mathbf{z}|\mu \sim \mathcal{N}(0,\sigma^2)$. When σ is small, \mathbf{z} can be approximately treated as $\mathcal{N}(0,1)$. $z^{(i)}$ and $\mu^{(j)}$ are independent for $i \neq j$, hence $z^{(i)} - \mu^{(j)} \sim \mathcal{N}(0,2)$, and for any t > 0, we can estimate the probability of $|z^{(i)} - \mu^{(j)}| < t$ by

$$P(|z^{(i)} - \mu^{(j)}| < t) = \frac{t}{2} + O(t^2)$$
(17)

See a proof in Appendix 4.

Generalized to D-dimension, the probability $P(|z^{(i)}-\mu^{(j)}| < t)$ would be $\frac{t^D}{2^D} + O(t^{D+1})^2$. Now, for the case $q(z_k^{(i)}|n^{(j)})$ being large, it happens only if $|z^{(i)}-\mu^{(j)}| < t$ and $t \leq 3\sigma$ (since the probability of normal distribution outside 3 standard deviation is very small). When $\sigma=0.1$, the probability of such cases to happen is $O(10^{-D})$. This means, when $i\neq j$, the number of such cases belongs to binomial distribution with $p=O(10^{-D})$ and n less than batch-size. While batch-size usually is less than 10^3 , such cases can be ignored if $D\geq 5$ (both mean and variance are small). Therefore, we can assume $q(z_k^{(i)}|n^{(j)})$ is small for all $i\neq j$.

Thus,

$$q(z_k^{(i)}|n^{(i)}) = O(1), \quad q(z_k^{(i)}|n^{(j)}) = o(1),$$

and

$$TC(\mathbf{z}) = \mathbb{E}_{q(z)} \left[\log \frac{q(z)}{\prod_{k} q(z_{k})} \right]$$

$$= \mathbb{E}_{q(z,n)} [\log q(z)] - \mathbb{E}_{q(z,n)} [\log \prod_{k} q(z_{k})]$$

$$\approx \frac{1}{M} \sum_{i} \left(\log \frac{1}{M} \sum_{j} \prod_{k} q(z_{k}^{(i)} | n^{(j)}) - \log \prod_{k} \frac{1}{M} \sum_{j} q(z_{k}^{(i)} | n^{(j)}) \right)$$

$$\approx \frac{1}{M} \sum_{i} \left(\log \frac{1}{M} \sum_{j=i} O(1) - \log \prod_{k} \frac{1}{M} \sum_{j=i} O(1) \right)$$

$$\approx \frac{1}{M} \sum_{i} \left(\log O(\frac{1}{M}) - \log O(\frac{1}{M^{D}}) \right)$$

$$\approx O((D-1) \log M).$$

To see this, notice that the region within a hypersphere, $\{z^{(i)}:|z^{(i)}-\mu^{(j)}|< t\}$, is contained in the hyper-rectangle, $\{z^{(i)}:|z_k^{(i)}-\mu_k^{(j)}|< t,k=1\dots D\}$. Now, recall the assumption that $\mathrm{TC}(\mathbf{z})$ is small, implying the correlation among each components of \mathbf{z} is low. Hence, the probability of the hyper-rectangle can be estimated simply by the product of the probability of each component.

6. Sketched Proof of equation 13

Recall that the first dimension of $\boldsymbol{\mu}$ gets shutdown, i.e., $\boldsymbol{\mu}_0 \sim \mathcal{N}(0,\sigma_0)$, where $\sigma_0 \ll 1$, and $\boldsymbol{\mu}_{0-} \sim \mathcal{N}(0,\mathbf{Id}_{D-1})$. Then for any $t > \sigma_0$, $P(|z_0^{(i)} - \mu_0^{(j)}| < t)$ is O(1). For the rest of the dimensions, it reduces to (D-1)-dimension case (since true $TC(\mathbf{z})$ is small, all dimensions can be treated independently). Hence, $P(|z^{(i)} - \mu^{(j)}| < t)$ is approximately $\frac{t^{D-1}}{2^{D-1}} + O(t^D)$. Therefore, only probabilities with indices (i,j,0) and (i,i,k) where k>0 take some bounded values O(1) and the rest can be ignored (for batchsize M, if σ_0 is sufficiently small, then we can choose t such that $\frac{t^{D-1}}{2^{D-1}} \cdot M \ll 1$). Hence, $\frac{1}{M} \sum_j q(z_0^{(i)}|n^{(j)}) \approx \frac{1}{M} \sum_j O(1) \approx O(1)$, and

$$\begin{split} TC(\mathbf{z}) &= \mathbb{E}_{q(z)} \left[\log \frac{q(z)}{\prod_k q(z_k)} \right] \\ &\approx \frac{1}{M} \sum_i \log \frac{\frac{1}{M} \sum_j \prod_k q(z_k^{(i)} | n^{(j)})}{\prod_k \frac{1}{M} \sum_j q(z_k^{(i)} | n^{(j)})} \\ &\approx \frac{1}{M} \sum_i \log \frac{\frac{1}{M} \sum_j (q(z_0^{(i)} | n^{(j)}) \cdot \prod_{k > 0} q(z_k^{(i)} | n^{(j)}))}{\prod_{k > 0} \frac{1}{M} \sum_j q(z_k^{(i)} | n^{(j)})} \\ &\approx \frac{1}{M} \sum_i \log \frac{\frac{1}{M} \cdot O(1)}{\prod_{k > 0} \frac{1}{M} \cdot O(1)} \\ &\approx \log O(M^{D-2}) \\ &\approx O((D-2) \log M). \end{split}$$

The above argument can be easily generalized to the case of S-dimension shutdown till some integer $S \leq S_0 \in (0,D)$. One reason for $S_0 < D$ is that, the argument stops being true if $\frac{t^{D-S-1}}{2D-S-1} \cdot M \ll 1$ no longer holds. After all, it is unlikely for a model to represent data with all latent dimensions shutdown.

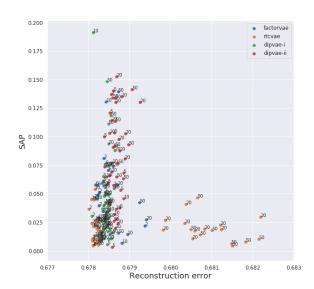
7. Experiments

Table 1. Model's hyperparameters.

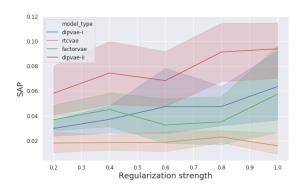
Model	Parameter	Values
FactorVAE	$\gamma = \beta$	[2, 6, 10, 20, 50]
RTC-VAE	β	[2, 6, 10, 20, 50]
DIP-VAE-I	λ_{od}	[2, 5, 10, 20, 50]
	λ_d	$10\lambda_{od}$
DIP-VAE-II	λ_{od}	[2, 5, 10, 20, 50]
	λ_d	λ_{od}

Table 2. Encoder and Decoder architecture. nc=number of channels

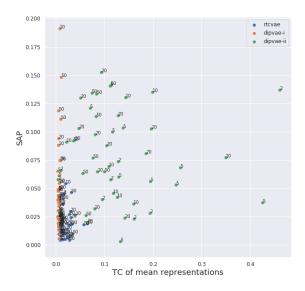
Encoder	Decoder	
Input: $nc \times 64 \times 64$	Input: \mathbb{R}^{10}	
4×4 conv, 32 ReLU, stride 2, padding 1	1×1 upconv, 512 ReLU, stride 1	
4×4 conv, 64 ReLU, stride 2, padding 1	4×4 upconv, 64 ReLU, stride 1	
4×4 conv, 64 ReLU, stride 2, padding 1	4×4 upconv, 64 ReLU, stride 2, padding 1	
4×4 conv, 64 ReLU, stride 2, padding 1	4×4 upconv, 32 ReLU, stride 2, padding 1	
4×4 conv, 512 ReLU, stride 1	4×4 upconv, 32 ReLU, stride 2, padding 1	
1×1 conv, 10, stride 1	4×4 upconv, nc ReLU, stride 2, padding 1	



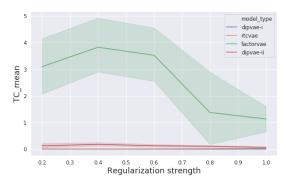
(a) The SAP score verses reconstruction error on dSprites. For RTCVAE, $\beta>10$ can affect the quality of reconstruction.



(c) The SAP score verses regularization strength on dSprites.

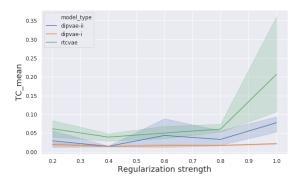


(b) The pair plot of TC_{mean} and SAP shows no strong correlation, indicating that factorized aggregated posterior alone does not necessarily lead to disentanglement.

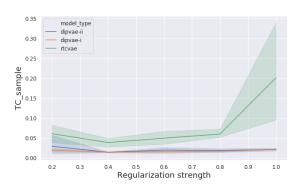


(d) Direct comparison of TC_{mean} of FactorVAE, DIP-VAEs and RTC-VAE on dSprites. Though both DIP-VAEs and RTC-VAE have low TC_{mean} , there is a difference in terms of factorized aggregated posterior.

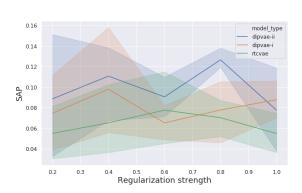
Figure 9. Scores evaluated on dSprites.



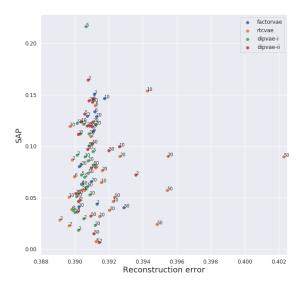
(a) TC_{mean} verses regularization strength.



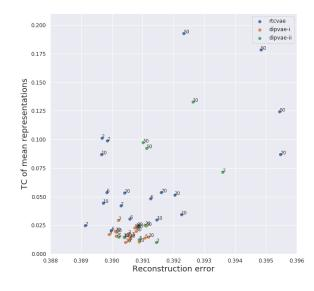
(b) TC_{sample} verses regularization strength.



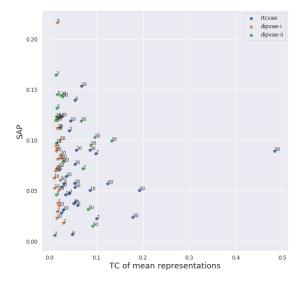
(c) The SAP score of models on Car3D under all regularization strength.



(d) SAP score verses reconstruction error.



(e) TC_{mean} verses reconstruction error. For RTCVAE, $\beta>10$ can affect the quality of reconstruction.



(f) Pairplot of SAP score and TC_{mean} shows no strong correlation, indicating factorizing alone does not guarantee disentanglement.

Figure 10. Scores evaluated on Car3D.

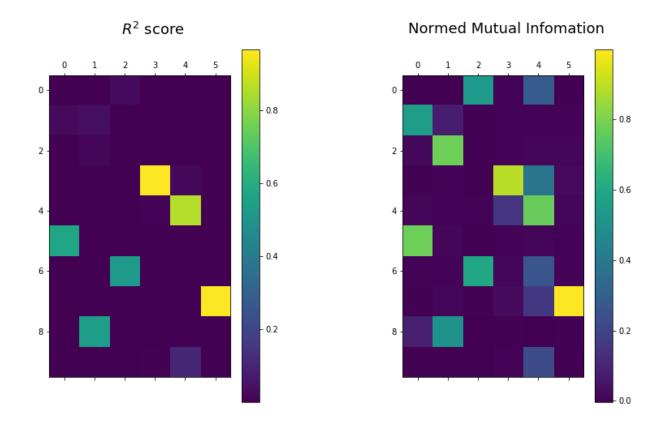
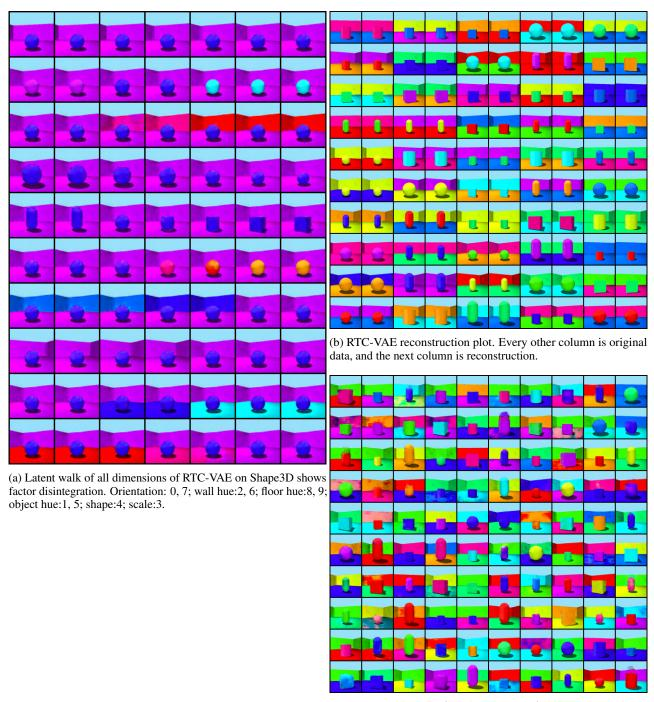


Figure 11. Evaluating a DIP-VAE-I model with \mathbb{R}^2 scores and normalized mutual information on Shape3D. Though DIP-VAEs do not guarantee factorized representation, they are also affected by non-compactness. (Left) \mathbb{R}^2 score seems not to show symptom of non-compactness because \mathbb{R}^2 score only captures the linear relation between random variables; (Right) Mutual information can capture nonlinear relation, so we see a lot more salient values on the right side. E.g., Factor 0, 1, 2, 4 all have small gaps between top 2 scores.



(c) Samples from latent space of RTC-VAE.

Figure 12. Experiment results from RTC-VAE with $\beta=10$

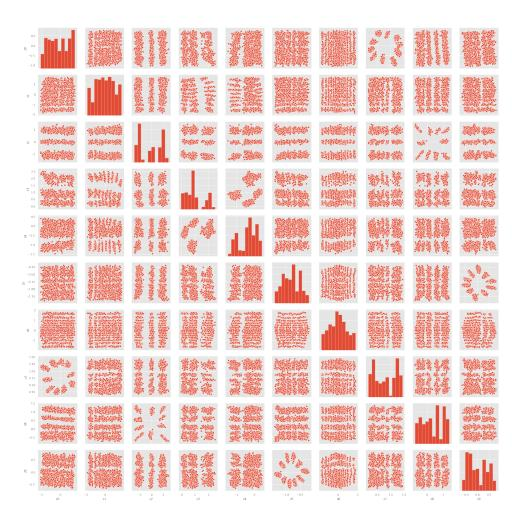


Figure 13. The pairplot of the mean representations of FactorVAE on 2000 samples of Shapes3D, $\gamma = 50$. Some dimensions show correlation, e.g. dim 4&3, and some are uncorrelated but not independent, e.g., dim 0&7, dim 2&8, dim 5&9 (refer to Section 5.4).

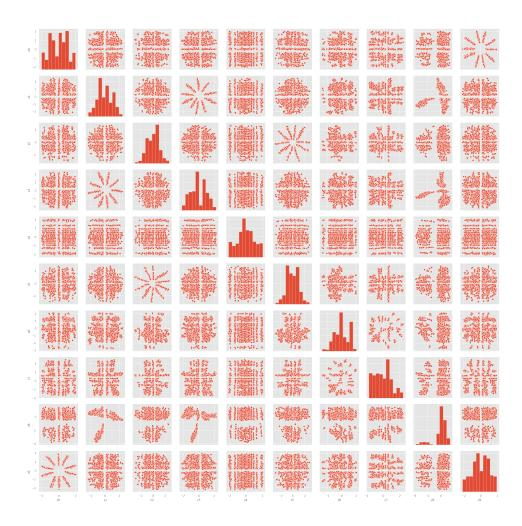


Figure 14. The pairplot of mean representations of DIP-VAE-I on 2000 samples of Shapes3D, $\lambda_{od}=20$. All dimensions are in discrete uncorrelated-like distribution. However, some dimensions are apparently not independent, e.g. dim 1&3, dim 1&3, dim 0&9, dim 2&5, dim 8&1,3, etc (refer to Section 5.2).

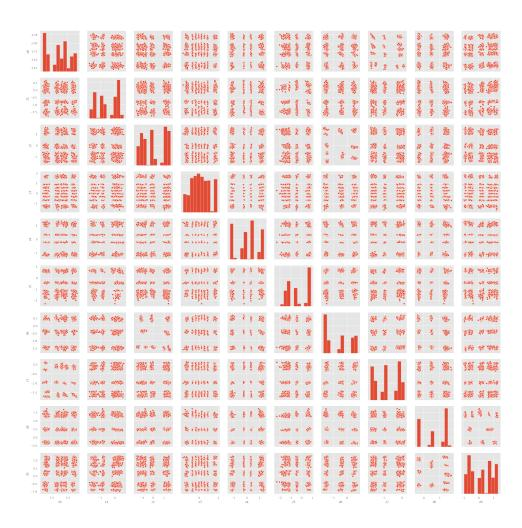


Figure 15. The pairplot of mean representations of RTC-VAE on 2000 samples of Shapes3D, $\beta = 20$. All dimensions are in discrete independent-like distribution (refer to Section 5.2).